Nano Hybrids *Online: 2012-08-22*
ISSN: 2234-9871, Vol. 2, pp 25-42
doi:10.4028/www.scientific.net/NH.2.25
© 2012 The Author(s). Published by Trans Tech Publications Ltd, Switzerland.

Structural and Thermal Properties of ACNT by Modified Deposition Method: Growth Time Approach

M.S. Shamsudin[1,2,a], M. Maryam[1,2,b], N.A. Asli[1,2,c], S.A.M. Zobir[1,2,d], M.A. Johari[1,2,e], S.F.M. Yusop[1,2,f], A.B. Suriani[1,2,g], S. Abdullah[1,2,h], S.Y.S. Yahya[1,2,i] and M. Rusop[1,3,j]

[1]NANO-SciTech Centre, Institute of Science;

[2]School of Physics and Material Studies, Faculty of Applied Sciences;

[3]NANO-ElecTronic Centre, Faculty of Electrical Engineering;

Universiti Teknologi MARA (UiTM), 40450 Shah Alam, Selangor D.E., Malaysia

[a]nanopizza@rocketmail.com, [b]mary_am_mohd@yahoo.com, [c]asnidasli@yahoo.com, [d]syzawn@yahoo.com, [e]amri_johari@yahoo.com, [f]shamsulfaez@gmail.com, [g]absuriani@yahoo.com, [h]saifollah@salam.uitm.edu.my, [i]syedy237@salam.uitm.edu.my, [j]rusop@salam.uitm.edu.my

Key words: carbon nanotube growth temperature, Modified deposition method, Camphor, Carbon nanotubes

Abstract. The knowledge of fabrication method plays an important role in the preparation of aligned carbon nanotubes (ACNT) from natural hydrocarbon feedstock. Here ACNT were successfully synthesized by two-stage catalytic chemical vapor deposition method using organic oil (camphor oil) as a precursor. Synthesis was carried out at a fixed growth temperature of 800 ^{o}C and in different growth time: 10, 20, 30, 40, 50 and 60 minutes. The optimized condition for the growth of ACNT produced a small amount of by-product amorphous carbon and highly uniform crystal structure. The experimental results demonstrated that formation ACNT is also dependent on the growth time. The nanotubes were characterized by field emission scanning electron microscopy and micro-Raman spectroscopy. Thermal properties were evaluated by thermogravimetric analysis.

This article is an open access article under the terms and conditions of the Creative Commons Attribution (CC BY) license
(https://creativecommons.org/licenses/by/4.0)

Introduction

Nearly twenty years after its discovery [1], carbon nanotubes (CNT) have gained tremendous attention in the science and engineering community due to their outstanding electronics and structural properties. In general, single-walled CNT (SWCNT) and multi-walled CNT (MWCNT) made of coaxial graphene sheet and/or sheets respectively. The most important apparatus developed to produce CNT include arc discharge [2], laser ablation [3] and chemical vapor deposition (CVD) [4]. Based on literature reviews, each method has its own merits and limitations [5]. The production process also influences the diameter, length and chirality of the nanotubes. Among the variety of synthesis approaches, CVD is the most suitable apparatus due to upward scalability and offers the benefits of the use of solid, gaseous and liquid carbon precursors.

Camphor Oil is obtained during the process of extraction of Camphor from Camphor Trees (Cinnamonum Camphora and also Dryobalanops Camphora). It can also be synthetically produced from oil of turpentine. Camphor oil is a tree product, which abundantly grows in almost all sub-tropical countries. So, it is a non-toxic and user-friendly starting material for growing CNT [6,7], as compared to precursors obtained from petrochemicals. This paper describes the formation of ACNT using a two-stage catalytic CVD method with iron (Fe) catalytic clusters deposited on silicon-based (Si) substrate. ACNT has more advantages over non-aligned CNT in many applications [8]. This ability, including the control over the individual ACNT diameter, aspect ratio, orientation, crystallinity and low defect level, would allow the exploitation of their exceptional structural and thermal properties [9].

Experimental Description

The details of experimental setups are as follows. In the literature plain p-type Si wafer was used as a supporting substrate for the formation of nanotubes [10]. Here also we used p-type Si substrate as received. The optimized ratio of ferrocene relative to camphor oil was 10 % w/v (weight-volume

ratio) [11] placed in different alumina boats and these two boats were positioned side by side [12] inside a quartz tube placed in the first chamber of a two-stage catalytic CVD apparatus. 2 cm x 2 cm Si substrate was mounted on another Al_2O_3 boat in the second chamber of the furnace as illustrated in Fig. 1 a). Then the system was continuously purged with nitrogen at 15 sccm (denotes cubic centimeter per minute at STP). After 10 minutes (to remove any gaseous impurities before increasing the temperature) the temperature of the first chamber of the furnace was raised to 180 ^{o}C and the temperature of the second chamber was maintained at 800 ^{o}C. In the first chamber sublimation and the vaporization process occurred to the ferrocene and camphor oil and the vapor flows with the nitrogen into the second chamber, where the temperature was maintained at 800 ^{o}C and the nanotubes were deposited on Si substrate in different time period i.e. at 10, 20, 30, 40, 50 and 60 minutes. Once the ACNT growth time completed the furnace was maintained at this temperature for 30 minutes and then was cooled down to room temperature under the nitrogen ambient, known as thermal annealing process [13]. The thermal annealing process was not only modified their structural features, but also eliminating defects and impurities.

The features of the synthesized ACNT (as in Fig. 1 b)) were analyzed by using field emission scanning electron microscope, FESEM originally designed by (JEOL, JSM-6700-F) and also by high resolution transmission electron microscopy (HRTEM) micrograph was obtained in a (FEI, Technai G2 20s Twin) at 200kV. Micro-Raman spectrometer (HORIBA JOBIN YVON, LabRam HR 800) with Ar^+ as a laser line at 514 nm wavelength. Thermal properties of the ACNT were investigated using a Perkin Elmer, Pyris 1 TGA analyzed at a heating rate of 20 ^{o}C/min and under ambient condition. Perkin Elmer, 2400 CHNS/O Elemental Analyzer was used for CHNS/O analysis.

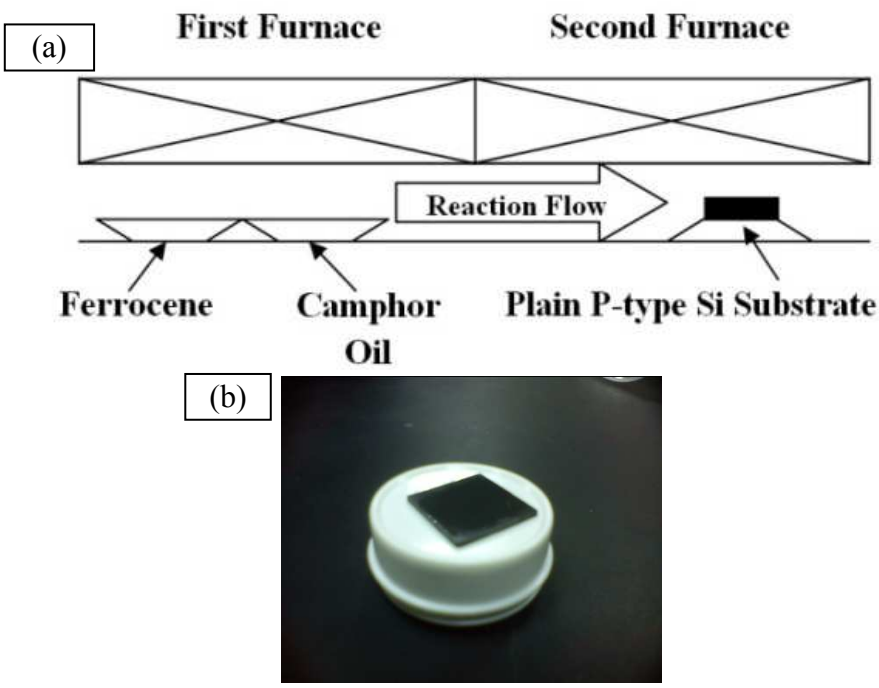

Fig 1. (a) Conceptual drawing of two-stage catalytic CVD, (b) CNT sample grown on Si substrate.

Results and Discussion

Fig. 2 displays FESEM micrographs of ACNT grown on the Si substrate at a fixed growth temperature of 800 ^{o}C in different time period. High magnification (100kX) of ACNT is shown at the top right of the images. This optimized temperature condition was selected from the literature [6,10-12]. In this experiment, the effect of different growth time from 10 to 60 minutes with increment of 10 minutes were analyzed. It was observed that amorphous carbon (a-C) was formed below 10 minutes, as the camphor oil did not fully decompose and may not form any ACNT growth below 10 minutes due to the low catalytic activity of iron (Fe). However, the density of ACNT was increased with a growth time period (see Fig. 2 a) to f)). This mechanism clearly indicates that at a lower growth time, the Fe particles just started to float and fall on the top surface of Si substrate [14]. There are some interactions between Fe particles to the top surface of Si substrate and may form an orange color thin layer. It was postulated that after reaching the hydrocarbon solubility limit in the Fe particles at an optimum growth time, as-dissolved carbon crystallizes started to form the tubular chain which is energetically stable. Similar finding was reported by A.B. Suriani et al. [15], these are known as either “tip-growth or base-growth model” [16]. In the same context, it was observed that

the longer as the growth time, the length of the ACNT continues to grow towards a certain lenght. This evidence also explains the general experience that ACNT growth is stopped once the catalytic activity is reduced. The average length of nanotubes was approximately 1, 3, 50, 100, 150, 200 μm shown in Fig. 2 a), b), c), d), e) and f) respectively. In increasing the growth time, nanotubes were produced in different diameter sizes. It has been found that the outer diameter size of the ACNT is bigger at a short growth time and in size decreases to less than 10 nm at a longer growth time. Here, it is speculated that the a-C layer surrounding ACNT is completely burned at a long growth time. As a result, the higher qualities of nanotubes have been produced. Subsequently, the energy dispersive X-ray was used to confirm the elements existing in the samples. As shown in the Fig. 2 g), several elements were detected such as carbon (C), oxygen (O), iron (Fe) and silicon (Si). The presence of C clearly indicates that formation and/or co-formation of the ACNT and a-C respectively exist in the resulting product, while Si detected is due to the substrate used to synthesize the ACNT. In addition, Fe and O are the main elements of the catalyst and co-catalyst.

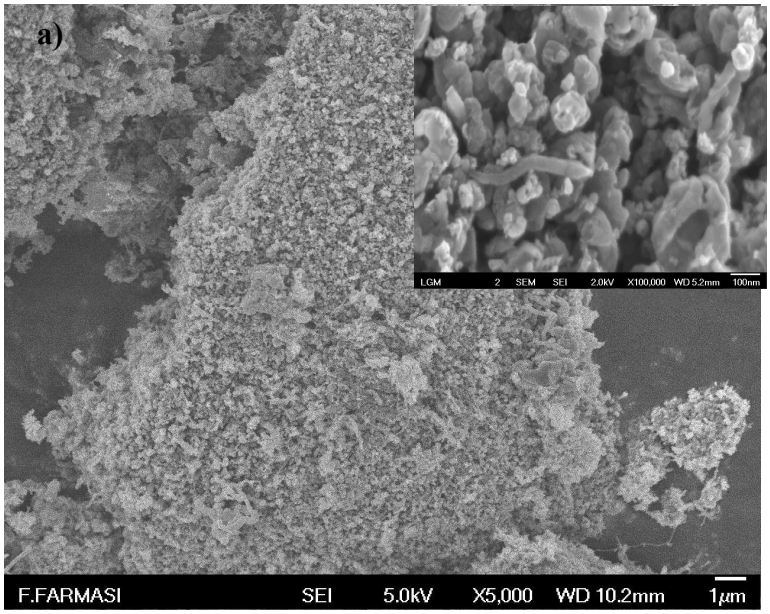

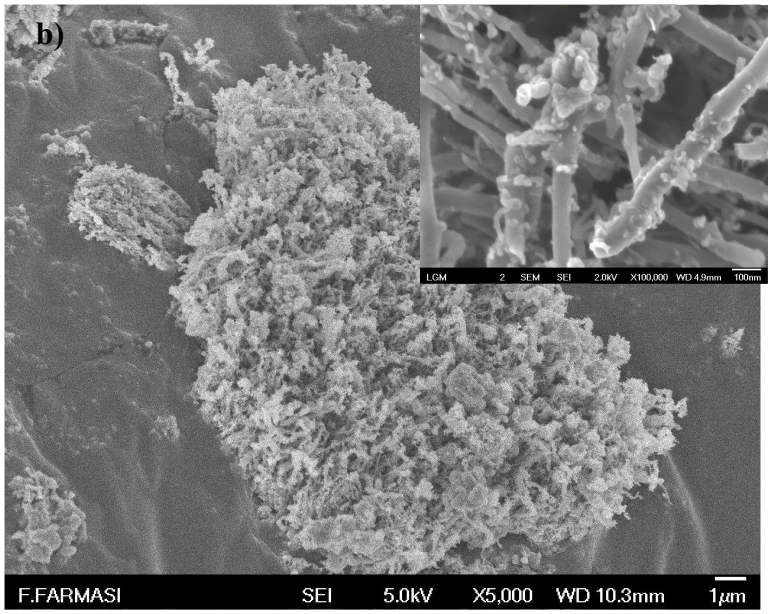
b)
LGM 2 SEM SEI 2.0kV X100,000 WD 4.9mm 100nm
F.FARMASI SEI 5.0kV X5,000 WD 10.3mm 1μm

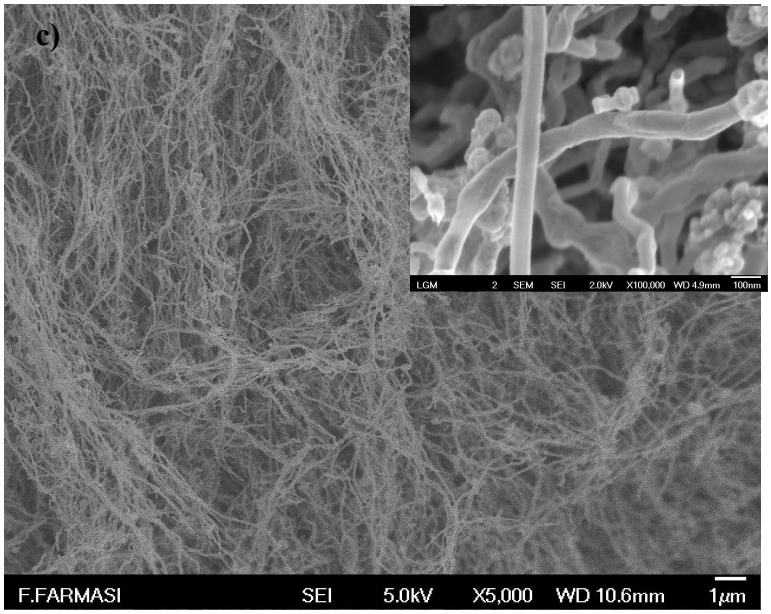
c)
LGM 2 SEM SEI 2.0kV X100,000 WD 4.9mm 100nm
F.FARMASI SEI 5.0kV X5,000 WD 10.6mm 1μm

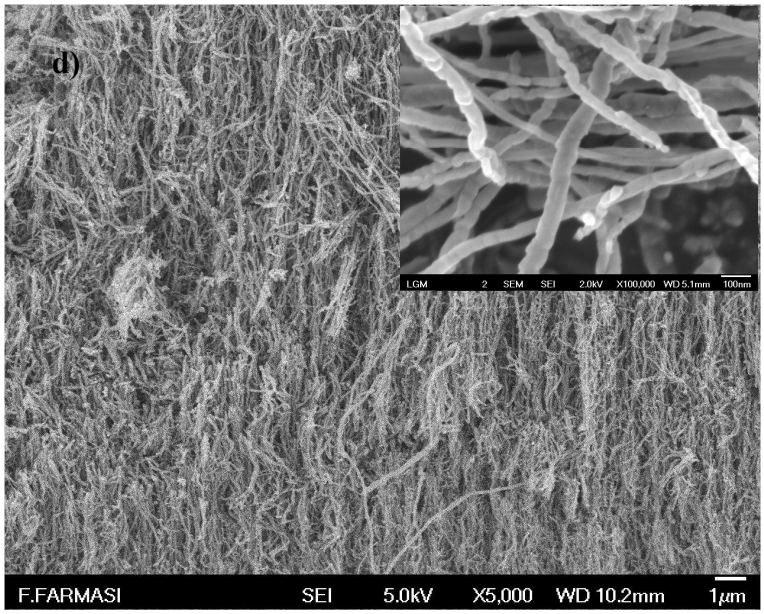
d)
LGM 2 SEM SEI 2.0kV X100,000 WD 5.1mm 100nm
F.FARMASI SEI 5.0kV X5,000 WD 10.2mm 1μm

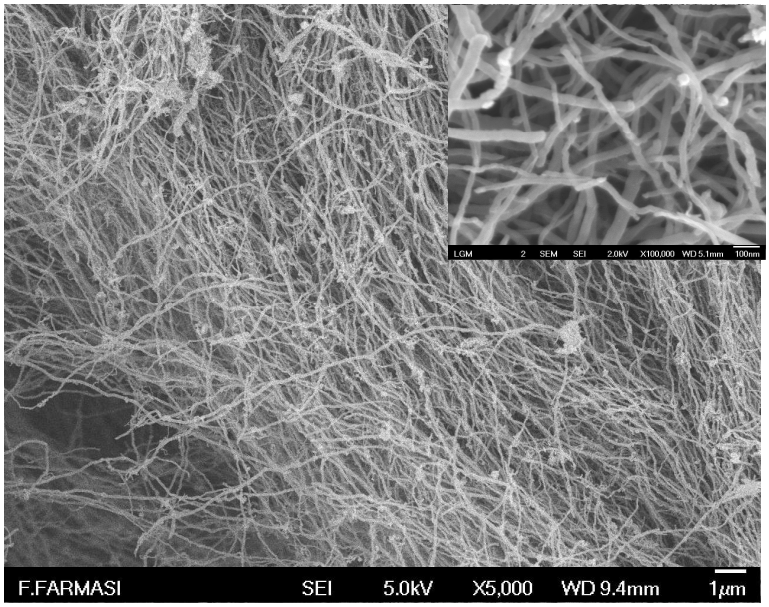
LGM 2 SEM SEI 2.0kV X100,000 WD 5.1mm 100nm
F.FARMASI SEI 5.0kV X5,000 WD 9.4mm 1μm

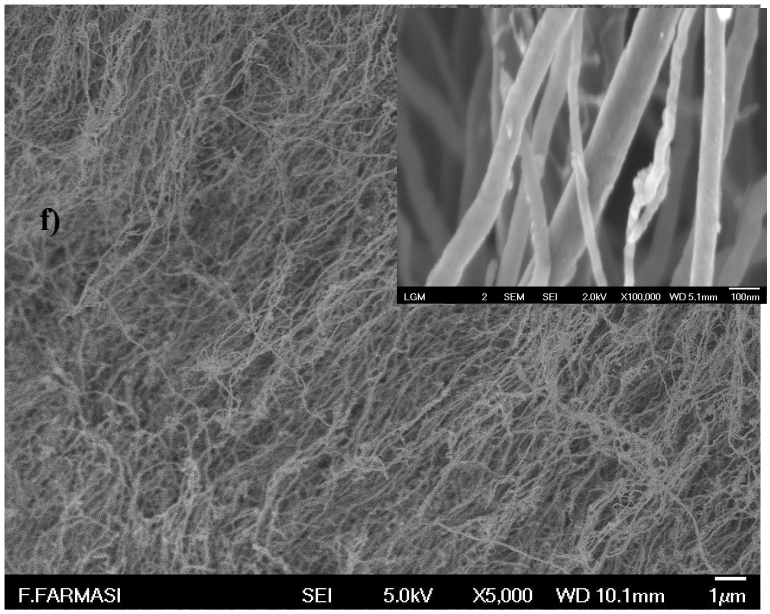

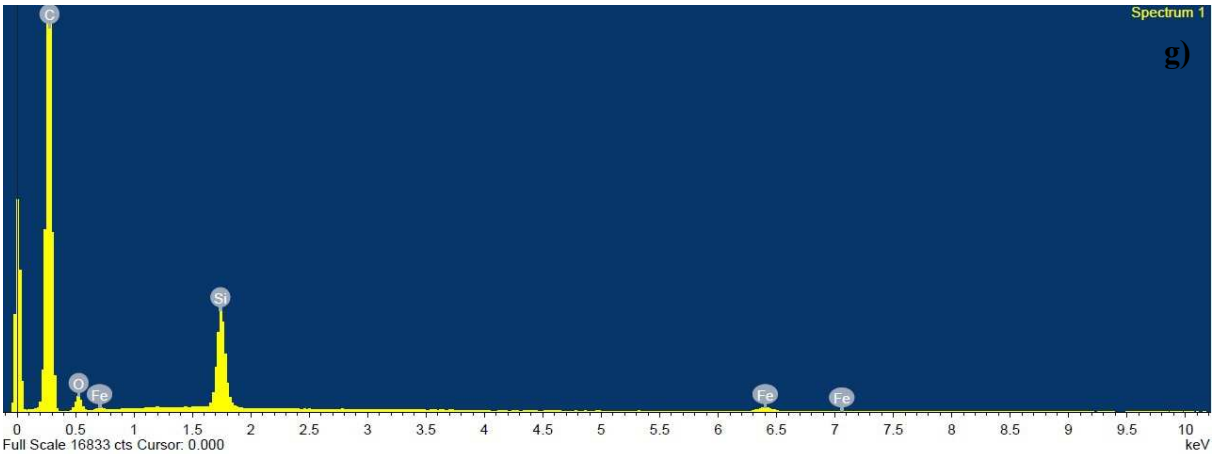

Fig. 2. FESEM micrographs of ACNT on the Si substrate at different growth time: a) 10, b) 20, c) 30, d) 40, e) 50 and f) 60 minutes. g) EDX analysis of ACNT.

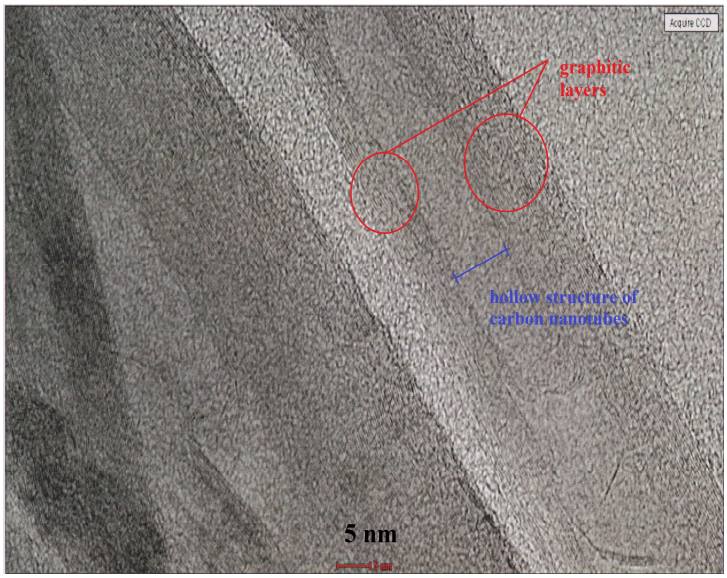

Fig. 3. HRTEM image of ACNT at 60 minutes growth time.

HRTEM image, as in Fig. 3, indicates the nature of the CNT at higher magnification and internal hollow structure was detected at the center of the CNT. Low surface impurities were found mostly due to less a-C deposited on its outer surface. Homogeneous and aligned graphitic layers indicates high crystallinity of ACNT. The appearance of the unwanted Fe particles can be seen in the ACNT; however, the amount is relatively low.

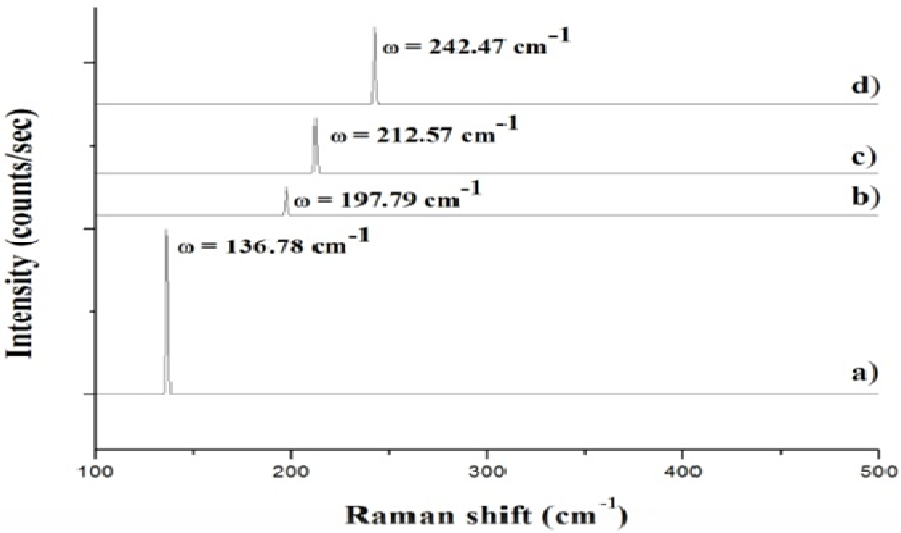

Fig. 4. Typical micro-Raman spectra of ACNT for RBM at different growth time: a) 30, b) 40), c) 50 and d) 60 minutes.

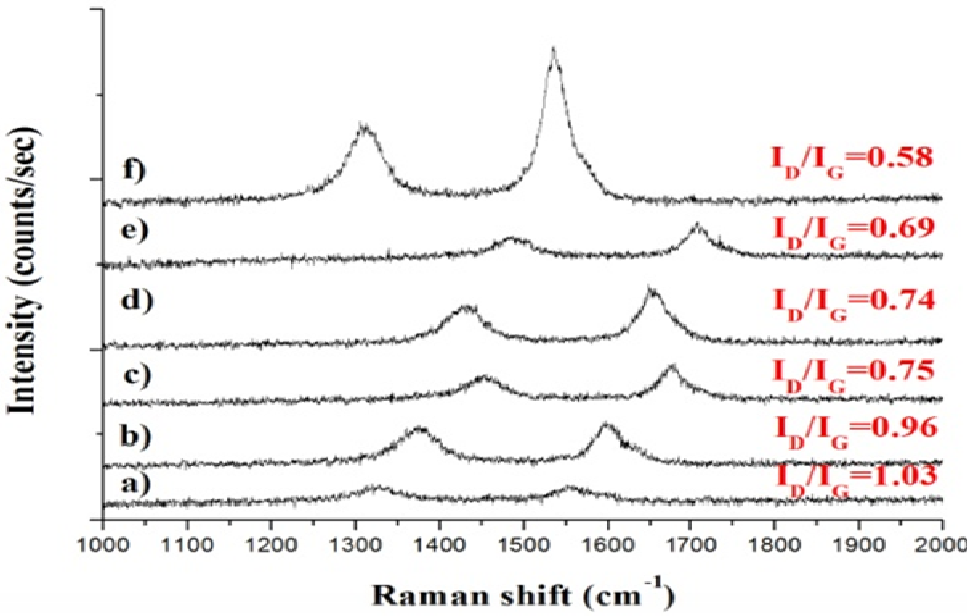

Fig. 5. Typical micro-Raman spectra of ACNT for TM at different growth time: a) 10, b) 20), c) 30, d) 40, e) 50 and f) 60 minutes.

The micro-Raman spectra were obtained at different growth times shown in Fig. 4 and Fig. 5, for radial breathing mode (RBM) and tangential mode (TM) in room temperature. The obvious RBM peak at the lower wave number region in between about 100 to 500 cm^{-1} were detected, indicating the existence of SWCNT [17]. RBM features correspond to the coherent vibration of the carbon atom in the radial direction of ACNT. According to Bandon's equation, the diameter, d of the SWCNT can be estimated from the sharp RBM peak position, ω as in equation 1 [18]. SWCNT was first grown by Dai et al. [19] from the disproportionation of carbon monoxide catalyzed by molybdenum nanoparticles. Later, SWCNT also was produced from several types of catalyst using various hydrocarbon precursors [20-22]. Based on the Fig. 4 analysis, the 30 minutes of growth time are required for the formation of SWCNT. SWCNT was not obtained at growth time less than 30 minutes due to the insufficient nucleation energy of Fe particles to catalyze the hydrocarbon decomposition efficiently. There are two general causes prevent the growth of SWCNT: i) size of Fe particles in the range of 5 to 20 nm form less-strained MWCNT and ii) size of Fe particles more than 100 nm acquire almost carbon microsphere with no sharp steps. That is why the carbon networks do not form CNT at all. In the micro-Raman spectra represented in Fig. 4, peaks were identified 136.78

cm^{-1} for 30 minutes, 197.79 cm^{-1} for 40 minutes, 212.57 cm^{-1} for 50 minutes and 242.47 cm^{-1} for 60 minutes growth time respectively. By increasing the growth time, RBM peak shifted to the right side which gave smaller SWCNT diameter size: 1.813 nm at 30 minutes, 1.254 nm at 40 minutes, 1.167 nm at 50 minutes and the lowest diameter size of nanotubes produced was 1.023 nm at 60 minutes as in Fig. 4 a), b), c) and d) respectively. This is the behavior of the quantum confinement effect because of the small diameter of SWCNT [23]. As a result, the lowest diameter size of nanotubes makes them ideal for any management applications [24].

$$d = \frac{248(cm^{-1}nm)}{\omega(cm^{-1})}. \quad (1)$$

As in the Fig. 5, the TM of ACNT analysis was conducted at higher wave number region between 1000 to 2000 cm^{-1} to evaluate the purity and degree of graphitization. Two prevalent peaks confederated with disorder-mode, (D-peak) and graphitic-mode, (G-peak) normally located at 1350 cm^{-1} and a range of 1500 to 1700 cm^{-1} respectively in CNT [25]. The G-peak position at 10, 20, 30, 40, 50 and 60 minutes growth time samples were observed at 1553, 1597, 1674, 1651, 1699 and 1536 cm^{-1} accordingly. The G-peak spectra of Fig. 5 a) and f) known as G_- feature (~1576 cm^{-1}) has a Breit-Wigner-Fano line shape, consistent with this location corresponds a metallic CNT. The G-peak spectra of Fig. 5 b), c), d) and e) known as G_+ feature (~1594 cm^{-1}), however, the wave number was shifted to the higher region has the Lorentzian line shape characteristic of the semiconducting CNT [26]. This finding proves that geometrical deformation of CNT affects to its band structure. But no specific method for chirality control of a ACNT has been developed [27] till date. It is reasonable to question whether it is either semiconducting or metallic CNT. A similar report was also found in the literature [28] that the frequency shift of G-peak, might be due to G_+ and G_- feature are associated with carbon atom vibrations along the nanotube axis and vibrations of carbon atom along the circumferential direction respectively. The appearance of the D-peak continues in this region for all samples as in Fig. 5 a) to f). In general, the intensity of D-peak indicates the first order of zone-boundary photon emission by scattering of an electron resonantly to evaluate the defect that break basic symmetries of graphene plane. The D-peak position at 10, 20, 30, 40, 50 and 60 minutes growth time samples were observed at 1321, 1374, 1452, 1429, 1480 and 1310 cm^{-1} respectively.

The defect level of ACNT can be obtained by comparing the integrated intensity ratio of D-peak after G-peak (I_D/I_G) as in Fig. 5. The I_D/I_G values at 10, 20, 30, 40 and 50 minutes growth time samples are 1.03, 0.96, 0.75, 0.74 and 0.69. From micro-Raman analysis, it is interesting to remark that the lowest I_D/I_G value of ACNT is about 0.58 reported at 60 minutes of growth time sample. Although 0.58 is not the best value, it is much lower than many recent reports of CNT [29-30]. The result implies that the I_D/I_G ratio decreased with long growth time. In order to evaluate this feature, this phenomenon could be correlated with the previous report, G-peak represents graphite-like sp^2-hybridized carbon while D-peak represents the amount of disordered sp^2-hybridized carbon and dominated with sp^3-hybridized carbon [31]. In this experimental result, the structure of ACNT is dominated by sp^2 bonding rather than sp^3 bonding at long growth time samples which indicates the enhancement of graphitic domain and reduction of bond angle disorder (heterojunction). Lowest I_D/I_G ratio indicates CNT has a little defect and high crystallinity [32].

The thermal sensitivity, TGA is widely used as a quality control tool in the material research and process development for the carbon and related materials [33]. The thermogram of the ACNTs are presented in Fig. 6. TGA profile was used to investigate the thermal variation of ACNT up to 1000 ^oC. All samples showed a similar oxidation behavior, with single step degradation except the ACNT sample grown at 30 minutes. The wt% loss of ACNT synthesized at 10, 20, 40, 50 and 60 minutes was 61.18, 62.72, 65.57, 68.22 and 70.64% respectively. There were approximately 38.82, 37.28, 35.16, 34.42 and 31.78 % residues for sample grown at 10, 20, 40 and 50 minutes respectively. The low residue left is for the ACNT sample grown at 60 minutes and it is about 29.36 %. Initial 7-10 % weight loss for the sample prepared in 30 minutes around 100 ^oC i n attributed to the oxidation of trace hydrocarbon impurities present in the sample [34]. We observed that the longer growth time favors ACNT formation and it also gives a high purity product [35]. For this reason, CHNS/O analysis could explain ACNT completely decompose into a rich composition of hydrocarbon containing C, H and O atoms. Notice that, it was estimated the C, H and O produced were 75, 5 and 3% pure respectively for 60 minutes synthesis time sample. The wt% remained might be due to presents of Fe cluster in the ACNT.

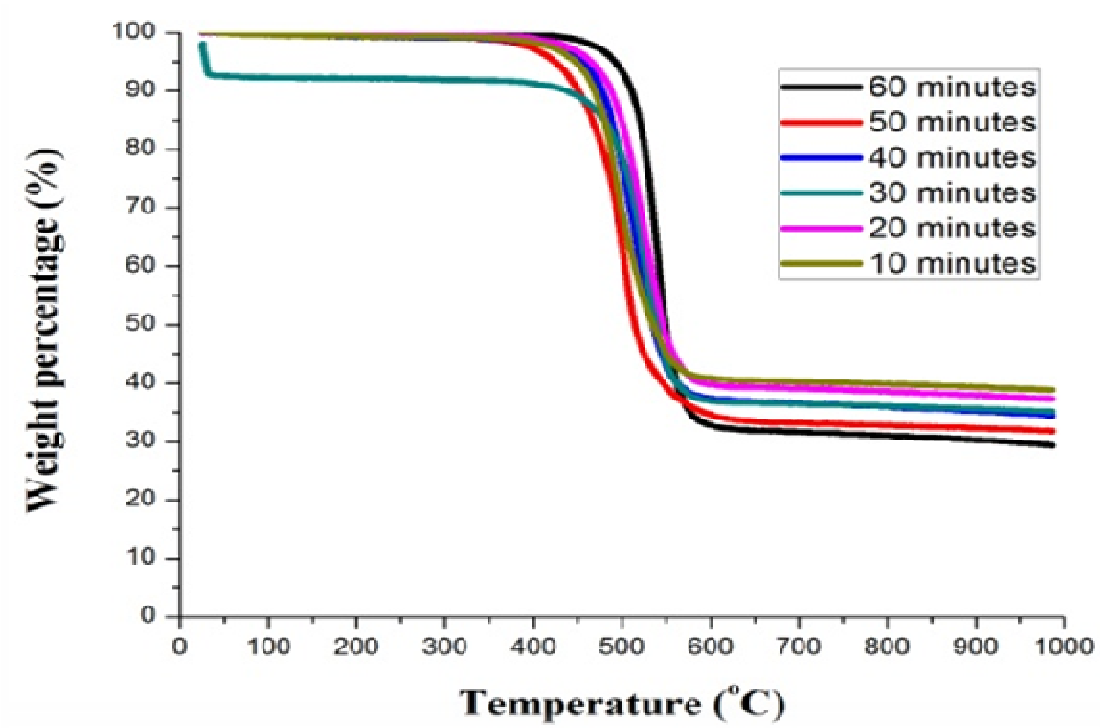

Fig. 6. Weight loss curves for ACNT synthesized by two-stage catalytic CVD over ferrocene catalyst at a different growth time.

Conclusions

This method may be favourable for promoting the enhancement properties factor in the growth of ACNT. Within this scope, it is expected that the possibility of growing large yield of nanotubes. The synthesis time was found to be one of the essential parameters that strongly affected the growth of ACNT. The formation of ACNT has been at the 60 minutes was found to be having better characteristic properties and the low coat non-toxic camphor oil can be a good source for large scale ACNT production.

Acknowledgements

This work was financially supported by the Malaysian Ministry of Higher Education through (Fundamental Research Grant Scheme and My Master scholarship program), Malaysian Ministry of Science, Technology and Innovation through (SciFund Grant), Research Management Institute through (Excellence Fund under contact no. 600-RMI/ST/DANA 5/3/Dst 435/2011) and the Institute of Graduate Studies through (Graduate Service Scheme). Special thanks to Mr. Abdul Karim Ishak from Microscopy Imaging Center (Faculty of Pharmacy, UiTM Puncak Alam) and Dr. Azira Abd Aziz (Malaysian Rubber Board) for providing FESEM and HRTEM facilities. We would like to express our gratitude to Mrs. Nurul Wahida Aziz, Mr. Mohd Azlan Jaafar and Mr. Salifairus Mohammad Jafar from NANO-SciTech Centre for their technical support. The authors acknowledge the constructive comments from anonymous reviewers.

References

[1] S. Iijima, T. Ichihashi, Single-shell carbon nanotubes of 1-nm diameter, Nature 363 (1993) 603-605.

[2] W. Krätschmer, L.D. Lamb, K. Fostiropoulos, D.R. Huffman, Solid C60: a new form of carbon, Nature 347 (1990) 354-358.

[3] Rahul Sen, S. Suzuki, H. Kataura, Y. Achiba, Growth of single-walled carbon nanotubes from the condensed phase, Chem. Phy. Lett. 349 (2001) 383-388.

[4] L. Philip, Jr. Walker, Carbon: An old but new material revisited, Carbon 28 (1990) 261-279.

[5] Y. Ando, X. Zhao, T. Sugai, M. Kumar, Growing carbon nanotubes, Mater. Today 7 (2004) 22-29.

[6] M. Kumar, Y. Ando, Single-wall and multi-wall carbon nanotubes from camphor-a botanical hydrocarbon, Diamond Relat. Mater. 12 (2003) 1845-1850.

[7] J. Tang, G.-Q. Jin, Y.-Y. Wang, X.-Y. Guo, Tree-like carbon grown from camphor, Carbon 48 (2010) 1545-1551.

[8] M. Mikami, K. Yamagiwa, T. Takeuchi, M. Saito, J. Kuwano, Synthesis of highly aligned carbon nanotubes in liquid phase, Key Eng. Mater. 350 (2007) 23-26.

[9] S. Wijewardane, Potential applicability of CNT and CNT/composites to implement ASEC concept: A review article, Solar Energy 83 (2009) 1379-1389.

[10] P. Szroeder, N.G. Tsierkezos, P. Scharff, U. Ritter, Electrocatalytic properties of carbon nanotube carpets grown on Si-wafers, Carbon 48 (2010) 4489-4496.

[11] M.S. Shamsudin, S. Abdullah, M. Rusop, Structural and thermal behaviors of iron-filled align carbon nanotubes formulated by two-stage catalytic chemical vapor deposition, Adv. Mater. Res. 364 (2012) 191-195.

[12] M.S. shamsudin, M.F. Achoi, M.N. Asiah, L.N. Ismail, A.B. Suriani, S. Abdullah, S.Y.S. Yahya, M. Rusop, An investigation on the formation of carbon nanotubes by two-stage chemical vapor deposition, Journal of Nanomaterials Vol. 2012 Art. ID 972126. doi: 10.1155/2012/972126.

[13] M. Kusunoki, T Suzuki, T Hirayama, N Shibata, Aligned carbon nanotube films on SiC (0 0 0 1) wafers, Physica B: Condensed Matter 323 (2002) 296-298.

[14] H. Ma, L. Pan, Y. Nakayama, Modelling the growth of carbon nanotubes produced by chemical vapor deposition, Carbon 49 (2011) 854-861.

[15] A.B. Suriani, A.A. Azira, S.F. Nik, R. Md Nor, M. Rusop, Synthesis of vertically aligned carbon nanotubes using natural palm oil as carbon precursor, Mater. Lett. 63 (2009) 2704-2706.

[16] J. Dijon, P.D. Szkutnik, A. Fourier, T. Goislard de Monsabert, H. Okuno, E. Quesnel, V. Muffato, E. De Vito, N. Bendiab A, Bogner, N. Bernier, How to switch from a tip to base growth mechanism in carbon nanotube growth by catalytic chemical vapour deposition, Carbon 48 (2010) 3953-3963.

[17] P. Liu, L. Liu, Y. Zhang, Alignment characterization of single-wall carbon nanotubes by Raman scattering, Physics Letters A 313 (2003) 302-306.

[18] Y. Zhao, T. Sugai, H. Shinohara, Y. Saito, Controlling growth and Raman spectra of individual suspended single-walled carbon nanotubes, J. Phys. Chem. Solids 68 (2007) 284-289.

[19] H. Dai, A.G. Rinzler, P. Nikolaev, A. Thess, D. T. Colbert, R. E. Smalley, Single-wall nanotubes produced by metal-catalyzed disproportionation of carbon monoxide, Chem. Phys. Lett. 260 (1996) 471-475.

[20] K. Hata, D.N. Futaba, K. Mizuno, T. Namai, M. Yumura, S. Iijima, Water-assisted highly efficient synthesis of impurity-free single-walled carbon nanotubes, Science 306 (2004) 1362-1364.

[21] Y. Murakami, S. Chiashi, Y. Miyauchi, M. Hu, M. Ogura, T. Okubo, S. Maruyama, Growth of vertically aligned single-walled carbon nanotube films on quartz substrates and their optical anisotropy, Chem.l Phys. Lett. 385 (2004) 298-303.

[22] S. Maruyama, R. Kojima, Y. Miyauchi, S. Chiashi, M. Kohno, Low-temperature synthesis of high-purity single-walled carbon nanotubes from alcohol, Chem. Phys. Lett. 360 (2002) 229-234.

[23] X. Zhao, Y. Ando, L.-C. Qin, H. Kataura, Y. Maniwa, R. Saito, Multiple splitting of **G**-band modes from individual multiwalled carbon nanotubes, Appl. Phys. Lett. 81 (2002) 2550-2552.

[24] R. Xiang, G. Luo, Z. Yang, Q. Zhang, W. Qian, F. Wei, Large area growth of aligned CNT arrays on spheres: Cost performance and product control, Mater. Lett. 63 (2009) 84-87.

[25] U. Ritter, P. Scharff, O.P. Dmytrenko, N.P. Kulish, Yu.I. Prylutskyy, N.M. Belyi, V.A. Gubanov, L.A. Komarova, S.V. Lizunova, V.V. Shlapatskaya, H. Bernas, Radiation damage and Raman vibrational modes of single-walled carbon nanotubes, Chem. Phys. Lett. 447 (2007) 252-256.

[26] B. Duong, S. Seraphin, L. Wang, Y. Peng, H. Xin, Production of predominantly semiconducting double-walled carbon nanotubes, Carbon 49 (2011) 3512-3521.

[27] R. Jasti, C.R. Bertozzi, Progress and challenges for the bottom-up synthesis of carbon nanotubes with discrete chirality, Chem. Phys. Lett. 494 (2010) 1-7.

[28] R. Rao, J. Reppert, R. Podila, X. Zhang, A.M. Rao, S. Talapatra, B. Maruyama, Double resonance Raman study of disorder in CVD-grown single-walled carbon nanotubes, Carbon 49 (2011) 1318-1325.

[29] S. Paul. S.K. Samdarshi, Carbon microtubes produced from coconut oil, New Carbon Materials 25 (2010) 321-324.

[30] S. Paul, S.K. Samdarshi, A green precursor for carbon nanotubes synthesis, New Carbon Materials 26 (2011) 85-88.

[31] M. Rusop, T. Kinugawa, T. Soga, T. Jimbo, Preparation and microstructure properties of tetrahedral amorphous carbon films by pulsed laser deposition using camphoric carbon target, Diamond Relat. Mater. 13 (2004) 2174-2179.

[32] M. Kumar, K. Kakamu, T. Okazaki, Y. Ando, Field emission from camphor-pyrolyzed carbon nanotubes, Chem. Phys. Lett. 385 (2004) 161-165.

[33] J. Madarász, G. Pokol, S. Kéki, M.T. Beck, Comparative thermogravimetric study of the oxidation of different carbons, Carbon 32 (1994) 1023-1024.

[34] B.P. Ramesh, W.J. Blau, P.K. Tyagi, D.S. Misra, N. Ali, J. Gracio, G. Cabral, E. Titus, Thermogravimetric analysis of cobalt-filled carbon nanotubes deposited by chemical vapour deposition, Thin Solid Films 494 (2006) 128-132.

[35] P. Moodley, J. Loos, J.W. Niemantsverdriet, P.C. Thüne, Is there a correlation between catalyst particle size and CNT diameter?, Carbon 47 (2009) 2002-2013.